eLIFE elifesciences.org

RESEARCH ARTICLE

Figures and figure supplements

Anterior insular cortex plays a critical role in interoceptive attention

Xingchao Wang *et al*

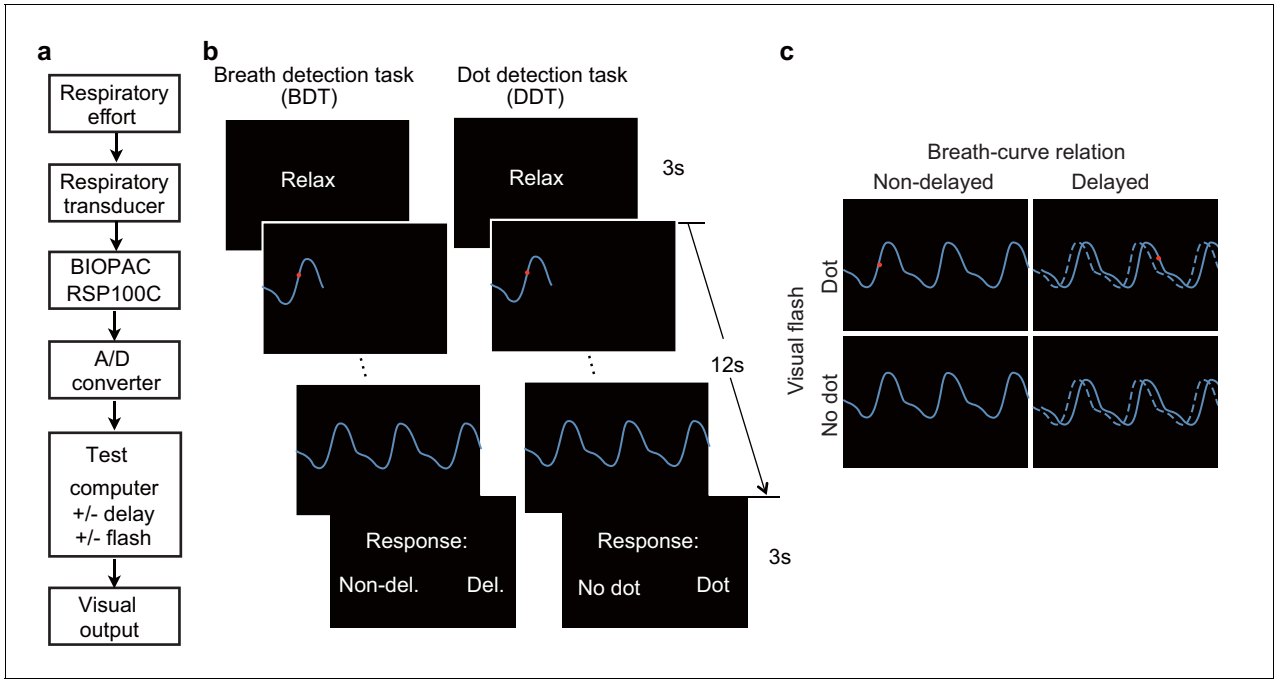

Figure 1. Experimental setup, trial structure of the tasks, and stimulus conditions. (**a**) The respiratory effort is converted into electronic signal changes using a respiratory transducer, amplified by BIOPAC, digitized using an A/D converter, and sent to the test computer for the final visual display as a dynamic breath curve, with or without a 400 ms delay. (**b**) This panel shows two trials for the breath detection task (BDT) and flash dot detection task (DDT) runs, respectively. Each trial begins with a 3 s blank display, followed by a 12 s display of respiratory curve presented with or without a 400 ms delay and with or without a 30 ms red dot flashed at a random position on the curve, and ends with a 3 s response window during which participants make a forced-choice button-press response to two alternative choices depending on the block type (BDT or DDT) to indicate whether the feedback curve is synchronous or delayed (for the BDT run) or whether a dot has appeared (for the DDT run). (**c**) The task represents a 2 × 2 × 2 factorial design with the factors of attention to breath or dot (block design), presence or absence of breath curve delay, and presence or absence of a dot flashed. The dashed line represents the actual breath curve, while the solid line represents the feedback breath curve displayed on the screen.

DOI: https://doi.org/10.7554/eLife.42265.002

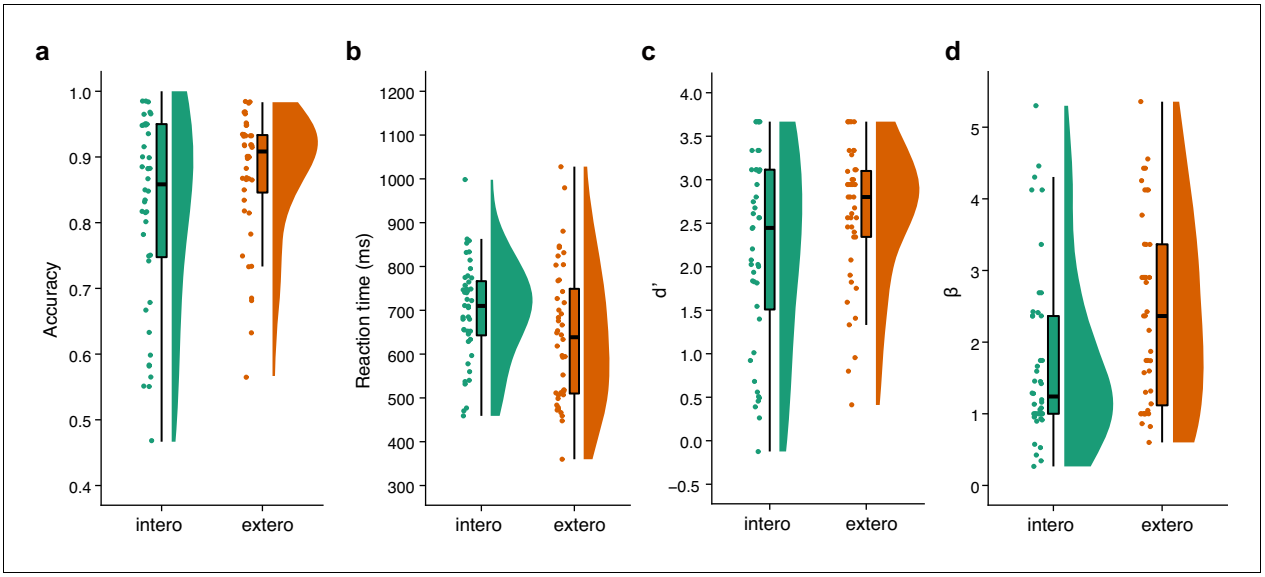

Figure 1—figure supplement 1. Raincloud plots visualizing the five-number summary (minimum, lower quartile, median, upper quartile, and maximum) for (**a**) accuracy, (**b**) reaction time, (**c**) d', and (**d**) β for the BDT and DDT tasks in the first sample of the fMRI study.
DOI: https://doi.org/10.7554/eLife.42265.003

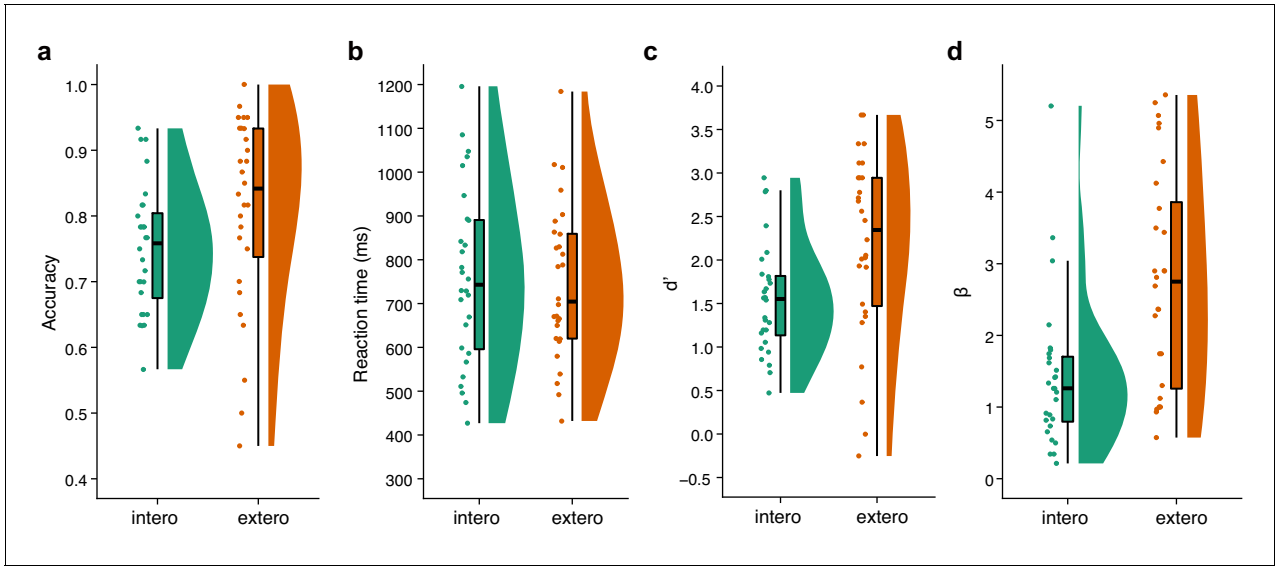

Figure 1—figure supplement 2. Raincloud plots visualizing the five-number summary (minimum, lower quartile, median, upper quartile, and maximum) for (**a**) accuracy, (**b**) reaction time, (**c**) d', and (**d**) β for the BDT and DDT tasks in the second sample of the fMRI study.

DOI: https://doi.org/10.7554/eLife.42265.005

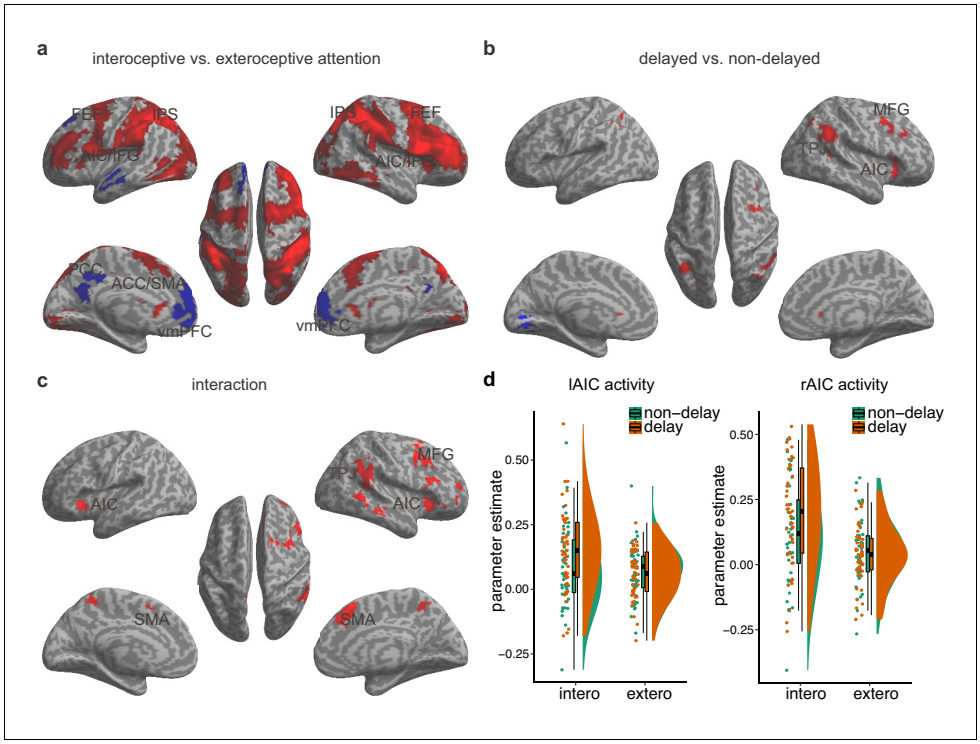

Figure 2. Main effects and the interaction effect of the whole brain analysis of the first sample. (**a**) Main effect of interoceptive vs. exteroceptive attention contrast (BDT vs. DDT). (**b**) Main effect of breath curve feedback condition (delayed curve vs. non-delayed curve). (**c**) Interaction between attention type and breath-curve feedback condition ([delayed – non-delayed] $_{BDT}$ – [delayed – non-delayed] $_{DDT}$). Here we showed the left AIC for the visualization of the seed for the ROI analysis in the second fMRI sample, although the cluster with 210 voxels did not survive GRF correction. Red color represents an increased activation; Blue color represents a decreased activation. (**d**) Activation of the left and the right AIC under the four task conditions, and the pattern of the interaction.

DOI: https://doi.org/10.7554/eLife.42265.010

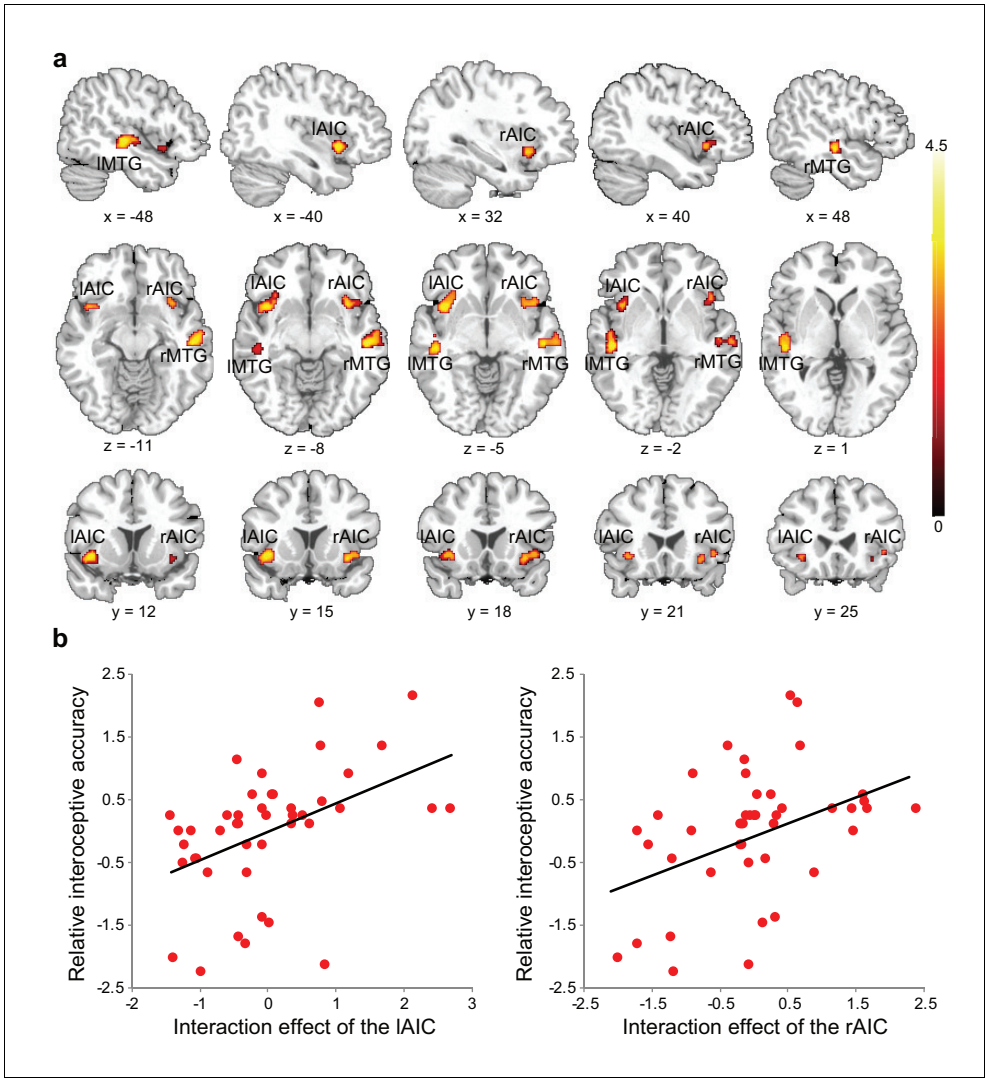

Figure 3. Relationship between brain activation and behavioral performance across participants. (**a**) This was revealed in a regression analysis of contrast images for the interaction between interoceptive attention deployment (BDT vs. DDT) and breath curve feedback condition (delayed vs. no-delayed), with performance accuracy on interoceptive and exteroceptive tasks as regressor-of-interest and covariate, respectively. AIC, anterior insular cortex; MTG, middle temporal gyrus. (**b**) Correlational patterns between the interaction effect of bilateral AIC activation and relative interoceptive accuracy. Data were normalized as z-scores.

DOI: https://doi.org/10.7554/eLife.42265.015

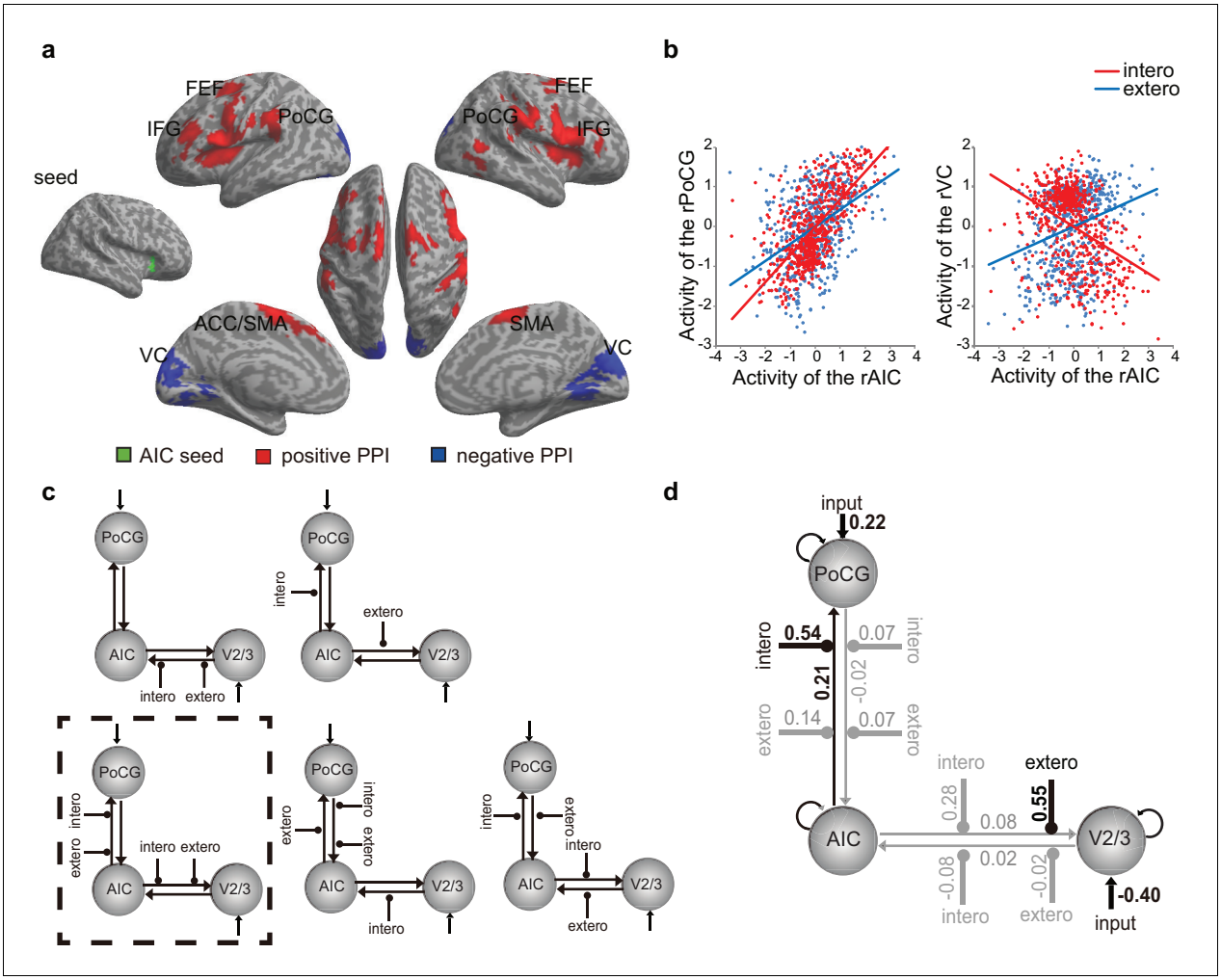

Figure 4. PPI and DCM results of the first fMRI sample. (**a**) Regions showing positive (red) and negative (blue) associations with AIC activation modulated by interoceptive attention relative to exteroceptive attention (BDT vs. DDT). (**b**) An increase in activation in the right AIC was associated with an increase in activation in the postcentral gyrus (PoCG) and a decrease in activation in the visual cortex (VC, V2/3) under the condition of interoceptive attention compared with exteroceptive attention. (**c**) Five base models generated by specifying possible modulations of interoceptive and exteroceptive attention (BDT and DDT) on the four endogenous connections between ROIs. The model surrounded by a rectangle in dashed-line indicates the winning model out of 52 variant models revealed by random-effects Bayesian model selection (BMS). (**d**) Intrinsic efferent connection from the AIC to the PoCG was significant. The modulatory effect of interoceptive attention (BDT) on the connection from the AIC to the PoCG was significant. The modulatory effect of exteroceptive attention (DDT) on the connection from AIC to V2/3 was significant (uncorrected).

DOI: https://doi.org/10.7554/eLife.42265.018

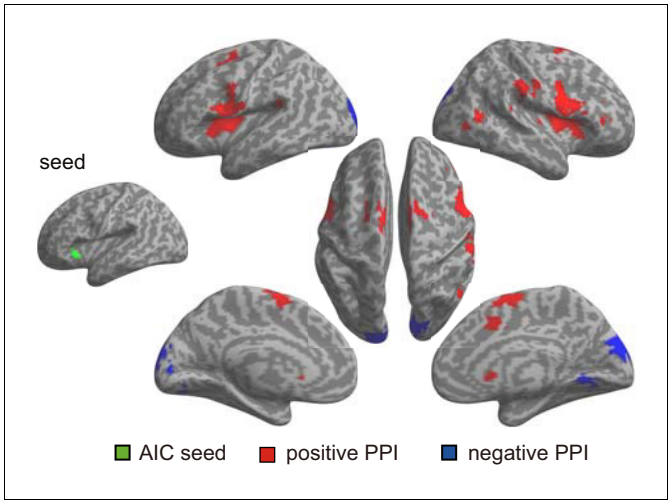

Figure 4—figure supplement 1. Regions showed positive (red) and negative (blue) association with the left AIC (as the seed) modulated by interoceptive attention relative to exteroceptive attention (BDT vs DDT) for the first fMRI sample.

DOI: https://doi.org/10.7554/eLife.42265.019

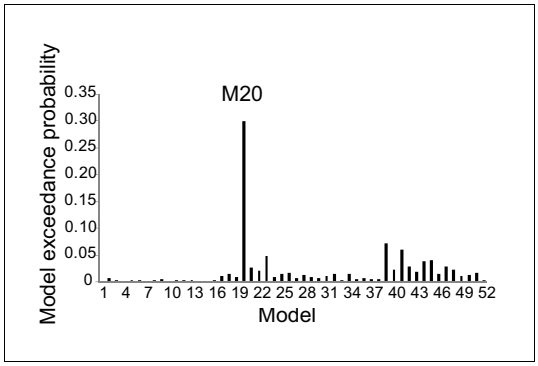

Figure 4—figure supplement 2. Exceedance probability of RFX BMS for the first fMRI sample. Across all 52 models, M20 outperformed the other models and thus was identified as the optimal model. M20 denotes the model with the modulatory effects of interoceptive and exteroceptive attention (BDT and DDT) exerting on the connection from the AIC to the PoCG and to the V2/3.

DOI: https://doi.org/10.7554/eLife.42265.020

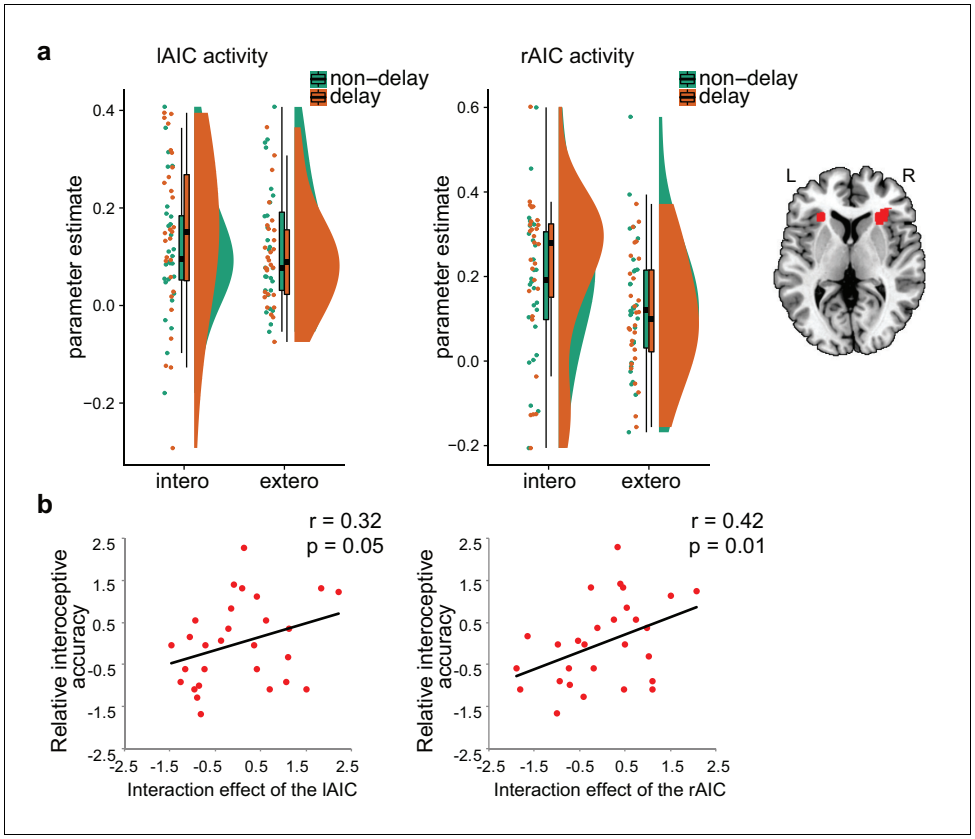

Figure 5. ROI results of the second fMRI sample. (**a**) ROI analysis of the parameter estimates of the left and the right AIC under the four experimental conditions. Raincloud plots were used for visualization. (**b**) Correlation between the interaction effect of bilateral AIC and relative interoceptive accuracy. The values of the variable in b were normalized as z-scores.

DOI: https://doi.org/10.7554/eLife.42265.023

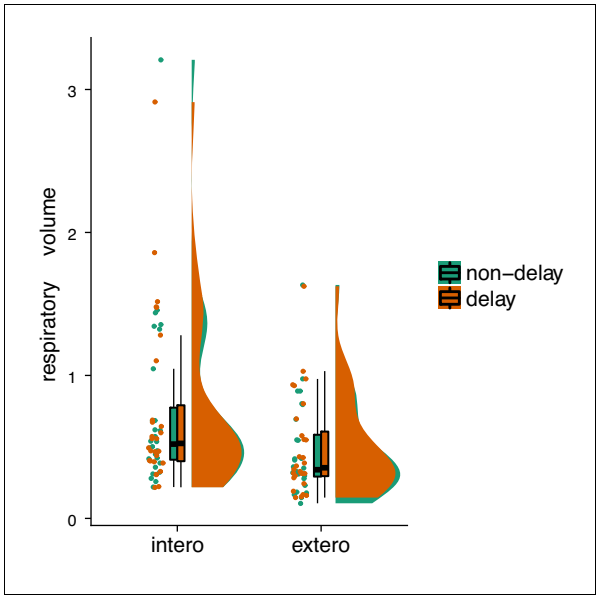

Figure 5—figure supplement 1. Raincloud plot visualization of respiratory volumes under the four experimental conditions from the second fMRI sample.
DOI: https://doi.org/10.7554/eLife.42265.024

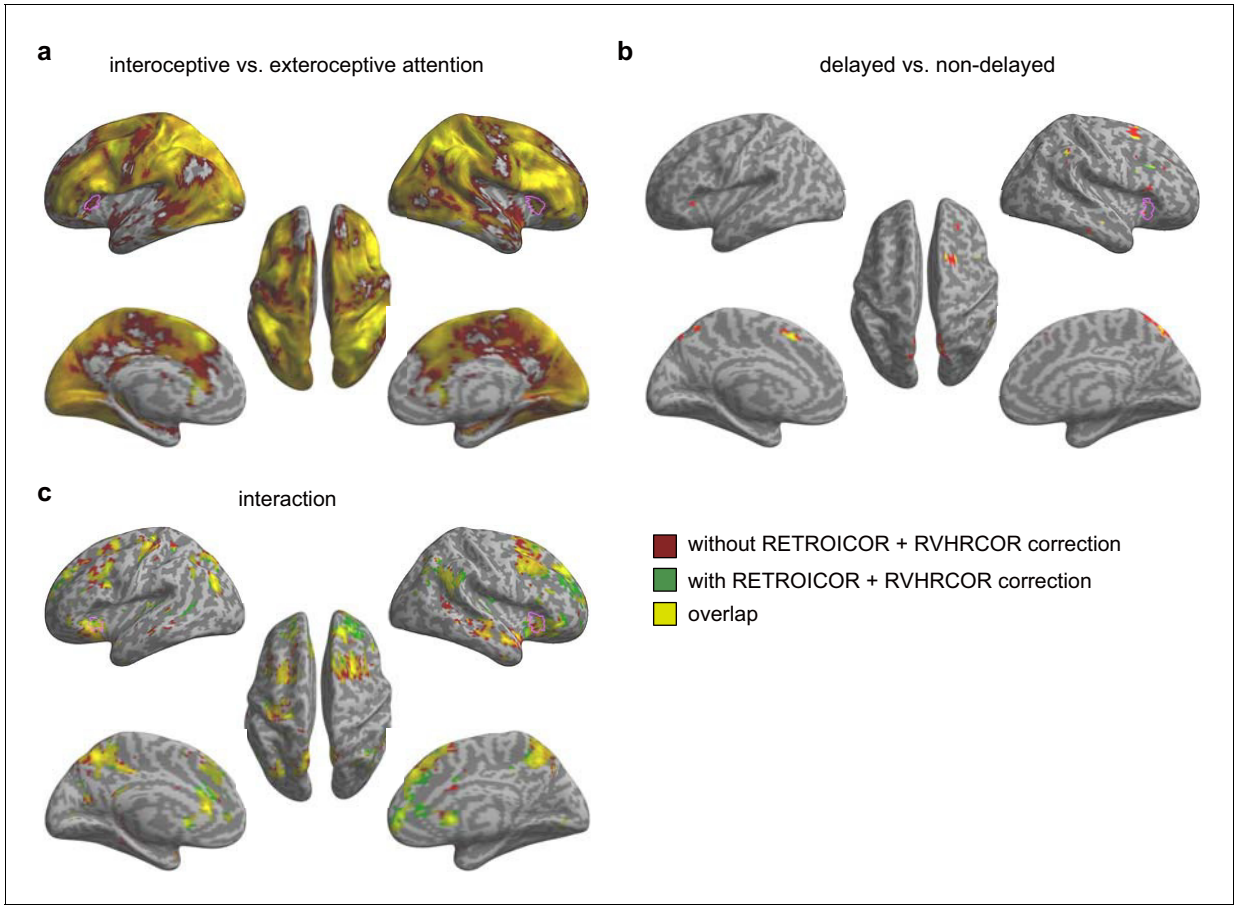

Figure 5—figure supplement 2. Activation maps without and with RETROICOR +RVHRCOR correction for the second fMRI sample. (**a**) Main effect of interoceptive vs. exteroceptive attention (BDT vs. DDT). (**b**) Main effect of breath curve feedback condition (delayed vs. non-delayed). (**c**) Interaction between attention type and breath-curve feedback condition ([delayed – non-delayed] $_{BDT}$ – [delayed – non-delayed] $_{DDT}$). Pink purple contours indicate corresponding activation in the first sample. We used an extremely liberal threshold of voxelwise $p<0.05$ for visualization.

DOI: https://doi.org/10.7554/eLife.42265.025

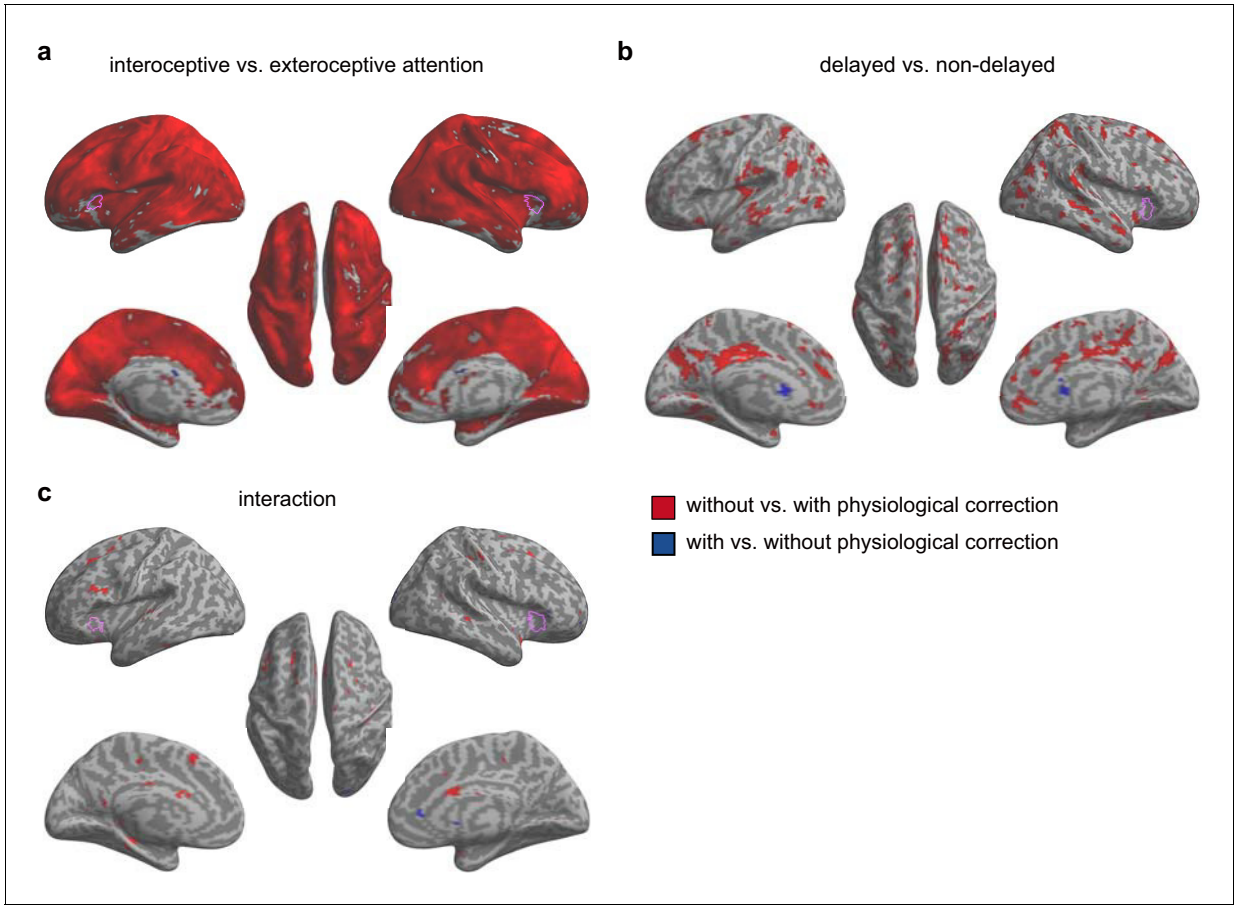

Figure 5—figure supplement 3. Paired t-test of beta maps obtained without and with RETROICOR + RVHRCOR correction for the second fMRI sample. The difference of the signals of the AIC between the analyses with and without physiological corrections was only evident under the main effect of interoceptive vs. exteroceptive attention (BDT vs. DDT), but not under the interaction contrast, confirming that the interaction effect of the AIC was not significantly impacted by the physiological noises. (**a**) Main effect of interoceptive vs. exteroceptive attention (BDT vs. DDT). (**b**) Main effect of breath curve feedback condition (delayed vs. non-delayed). (**c**) Interaction between attention type and breath-curve feedback condition ([delayed – non-delayed] $_{BDT}$ – [delayed – non-delayed] $_{DDT}$). Pink purple contours indicate corresponding activation in the first sample. We used an extremely liberal threshold of voxelwise $p<0.05$ for visualization.

DOI: https://doi.org/10.7554/eLife.42265.026

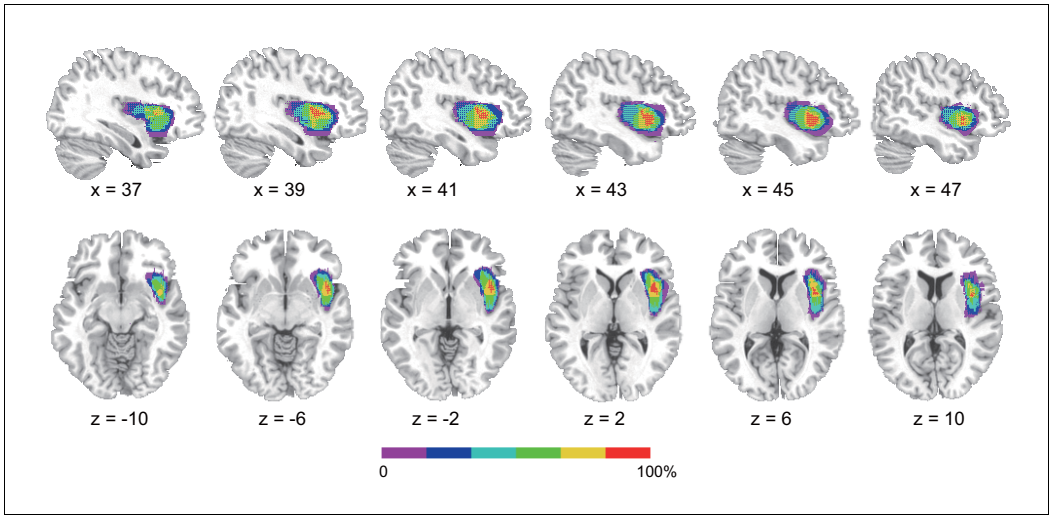

Figure 6. Reconstruction of anterior insular cortex lesions of six patients. Red color indicates 100% overlap. Left lesions were flipped to the right side to map the lesion overlap.

DOI: https://doi.org/10.7554/eLife.42265.028

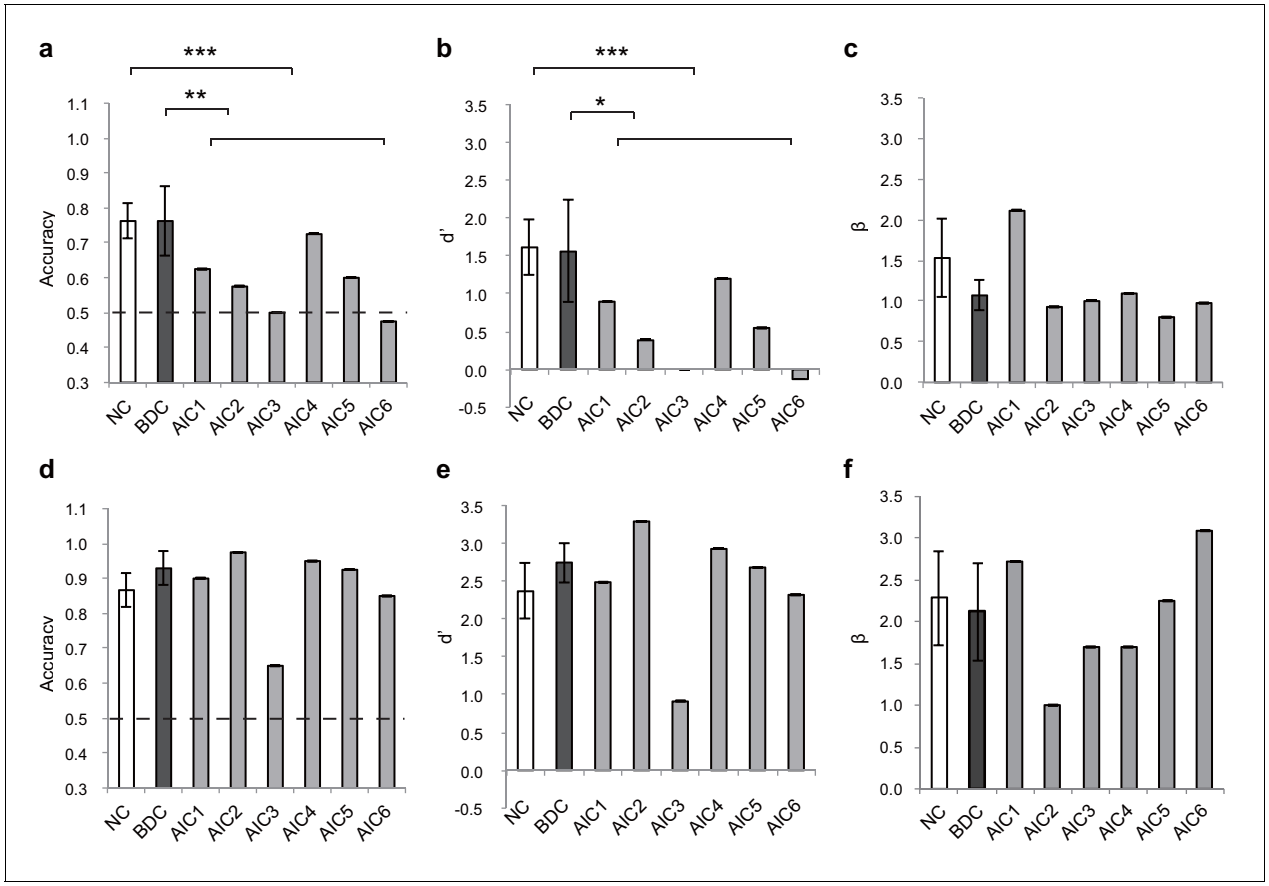

Figure 7. Behavioral results of the lesion study. (**a, b, c**) the interoceptive performance on the BDT, and (**d, e, f**) the exteroceptive performance on the DDT. On the BDT, patients with AIC lesions had significantly lower performance in accuracy and *d'* compared with the NC and BDC groups but did not show significant alteration in β during the BDT. On the DDT, patients with AIC lesions did not show significant abnormality in performance in accuracy, *d'*, and β compared with either the NC or BDC groups. NC, normal control; BDC, brain damage control. Dashed line: chance level. * $p < 0.05$; ** $p < 0.01$; *** $p < 0.001$.

DOI: https://doi.org/10.7554/eLife.42265.030